

ANALYSIS OF USING ACOUSTIC MICROSCOPY TO EVALUATE DEFECTS IN SPOT WELDING JOINTS

The article presents the possibilities of using acoustic microscopy to evaluate defects in resistance spot welding joints. For this purpose, the welded joints were made from two grades of aluminium plates EN AW5754 H24 and EN AW6005 T606, which were then subjected to non-destructive testing using acoustic microscopy and conventional destructive testing using traditional light microscopy techniques. Additionally, the study examined the influence of the typical contaminants found in industrial conditions on the quality of the joint.

Keywords: resistance spot welding, acoustic microscopy, aluminium, metallography

1. Introduction

Despite the development of many modern techniques for joining materials (e.g. laser welding [1]), resistance spot welding remains the most popular technique of joining in the automotive industry, railways and many other areas of industry. It has a number of characteristic advantages, the major of which include relatively low energy consumption, rapidity of making a single joint and the lack of need for additional materials. These facts are decisive for the general application of this technology. According to statistical data, about 2 billion spot welds are made in Poland every year [2]. The constant strive of designers and technologists to increase the reliability and reduce the costs of their products leads to a lot of interesting, innovative solutions. The evolution of resistance welding processes include both composite materials with ever-increasing operating characteristics, performance, and durability and the welding machines themselves [3], equipped e.g. in different types of control units.

In modern manufacturing systems, ensuring the highest quality of products is an important issue. Due to the large number of welds made e.g. in the construction of motor vehicles, inspecting every weld with the available manual application is rather inefficient and time-consuming. This caused a sudden demand for non-destructive techniques to test the mechanical properties of materials, composition, material structure and internal discontinuities.

One of the methods for examining the internal structure of spot welds with high spatial resolution after the welding process is scanning acoustic microscopy (SAM). Compared to an alternative technique of X-ray tomography, it is characterized by

simplicity, a high degree of safety as well as greater efficiency and speed. These factors combined with physical properties of ultrasounds (ex. reflection, refraction, absorption, dispersion) cause that scanning acoustic microscopy can be used for evaluation of welding joints, adhesive joints, surface conditions and material characterization [4-6]. Moreover, by using digital signal processing algorithms, it is possible to establish the anisotropic properties of the study material and its plastic properties. The following properties can be determined based on algorithms such as: correlation analysis, discrete Fourier transform, wavelet transform, and such processing operations as oversampling and nonuniform quantization.

Scanning acoustic microscopy requires high frequency ultrasonic transducer while using the acoustic lens focusing the ultrasonic beam, which produces the effect of object magnification, and concentrates the ultrasonic beam at the selected spot. It is assumed that the resolution of the acoustic microscope is half the wavelength of the ultrasonic transducer used. Typical frequency ranges of transducers are between 5-200 MHz [7]. Testing spot welds usually involve heads with a working middle frequency up to 50 MHz (typically its range is limited between 15-50 MHz). The use of higher frequency transducers increases the damping coefficient. An acoustic microscope can work in two ways: by echo or by passage (transmission). The testing of spot welds usually uses the echo method; therefore this method will be discussed in detail.

A typical scanning acoustic microscope consists of a propulsion system, which allows the movement of the transducer in the X, Y, Z axes; a generator and receiver system, which focuses the ultrasonic head, and an industrial PC with software

* WROCLAW UNIVERSITY OF TECHNOLOGY, DEPARTMENT OF MATERIALS SCIENCE, WELDING AND STRENGTH OF MATERIALS, 27 WYBRZEŻE WYSPIAŃSKIEGO STR., 50-370 WROCLAW, POLAND

Corresponding author: marcin.korzeniowski@pwr.edu.pl

enabling control of both the propulsion system and the ultrasonic block (gain system, the scope of observation, etc.). The drive block consists of a set of precision stepper motors which allow the movement of the head in 3 dimensions. These motors allow the movement in the Z axis (up and down) to remain constant during the scan and also serve to calibrate and accurately focus the ultrasonic beam.

In order to obtain a correct ultrasonic image (C-scan and B-scan of the spot weld area), it is necessary to put the sample in a plane perpendicular to the ultrasound beam.

If the acoustic microscope uses the immersion method, it is necessary to use a liquid (usually water) as a coupling medium. As a result, the ultrasonic beam is applied to the sample and then returns to the transmitter. In order to obtain proper coupling, it is necessary to eliminate air bubbles from the coupling fluid, which could disperse the ultrasonic beam and thus deform and bias the resulting ultrasound image.

With scanning acoustic microscopy, it is possible to acquire the following information on the spot weld:

- technological parameters of the joint: determining the diameter and shape of the welding nugget, the depth of electrode indentation,
- detection of internal and external discontinuities: cracks, voids, lack of welding and expulsion.

The detection of these technological parameters and discontinuities is possible by analyzing the differences in the amplitude and transit time of the ultrasonic wave generated by the ultrasonic transducer. The microscope has several modes of operation. Depending on the choice of the type of imaging and individual needs of the user, the greyscale may represent the transition time or the amplitude of the ultrasonic wave.

During the movement of the transducer with a focusing head over the sample surface, the ultrasound wave is alternately generated and received. While in the area outside the welding nugget, the ultrasonic wave is reflected from the water-top sheet boundary surface, from the sheet-sheet boundary and from the bottom sheet. This is characterized by a strong reflection on the sheet-sheet boundary, visible on the type A presentation (Fig. 1).

When the head is over the welding nugget, the ultrasound A-scan image shows 2 reflections (assuming that the nugget is homogeneous, without internal discontinuities), the first – from the water-top sheet boundary and the second – reflection from the other sheet. Compiling separate steps with suitably selected pulses of the A-scan in the X and Y planes, we will get a two-dimensional image of the scanned area, the so-called C-scan.

The microscope software allows tracking the amplitude or the transition time of any selected pulse (reflection from the water-top sample surface boundary), so the grey scale represents the amplitude or transit time of the ultrasonic wave (Fig. 2).

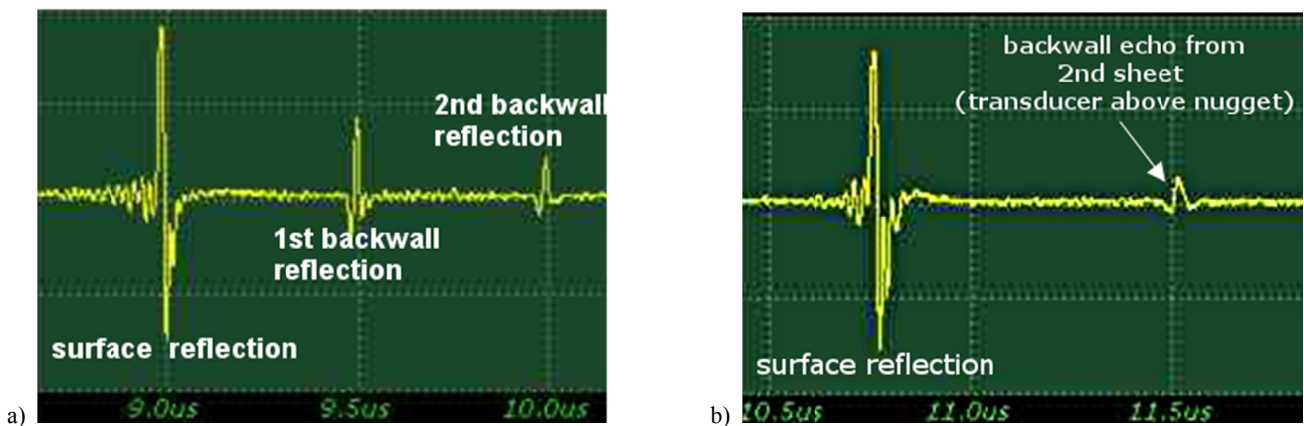


Fig. 1. A-scan image of the ultrasonic wave. Transducer outside the welding nugget (a), transducer above the welding nugget (b) [8]

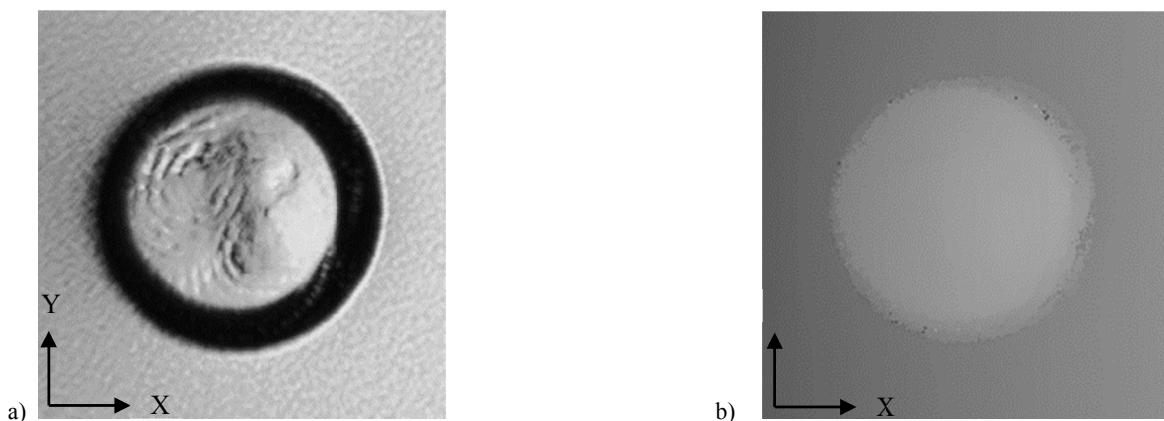


Fig. 2. Type C presentation of a spot weld, where the grey scale represents the amplitude-(a) and the transition time-(b) [8]

While calibrating the measuring system outside the welding nugget and setting the range to include the second reflection, a C-scan of the sheet-sheet boundary surface can be obtained. This solution is used to evaluate the diameter of the nugget, its shape and to detect internal discontinuities.

While recording differences in the transition time of an ultrasonic wave and the amplitude along the weld section, a cross-section of the object can be obtained, a so-called B-scan. In this image, the Y axis represents the transition time of the ultrasonic wave through the test material, and the X axis – the distance.

The principle of the B-scan image, assuming that the scope of observation only covers the sheet-sheet interface and the optional second reflection, is shown in Fig. 3.

By proceeding in a similar way, we can very accurately depict the profile of the spot weld surface along the selected section (Fig. 4). In this case, the scope of observation should include the first reflection. The disadvantage of precise measurement of the indentation depth may be due to difficulties associated with vertical positioning of the sample relative to the incident ultrasonic beam. Knowing the propagation speed of the ultrasonic wave in the material, it can be easily calculated the transition time into distance and thus assess the depth of any possible discontinuities.

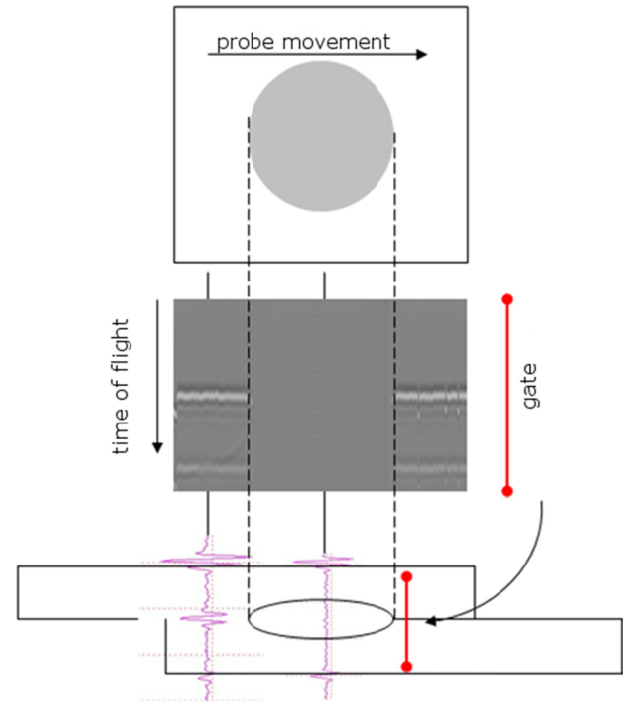


Fig. 3. Schematic presentation of the formation of a C-scan for scanning acoustic microscope. Author's own work

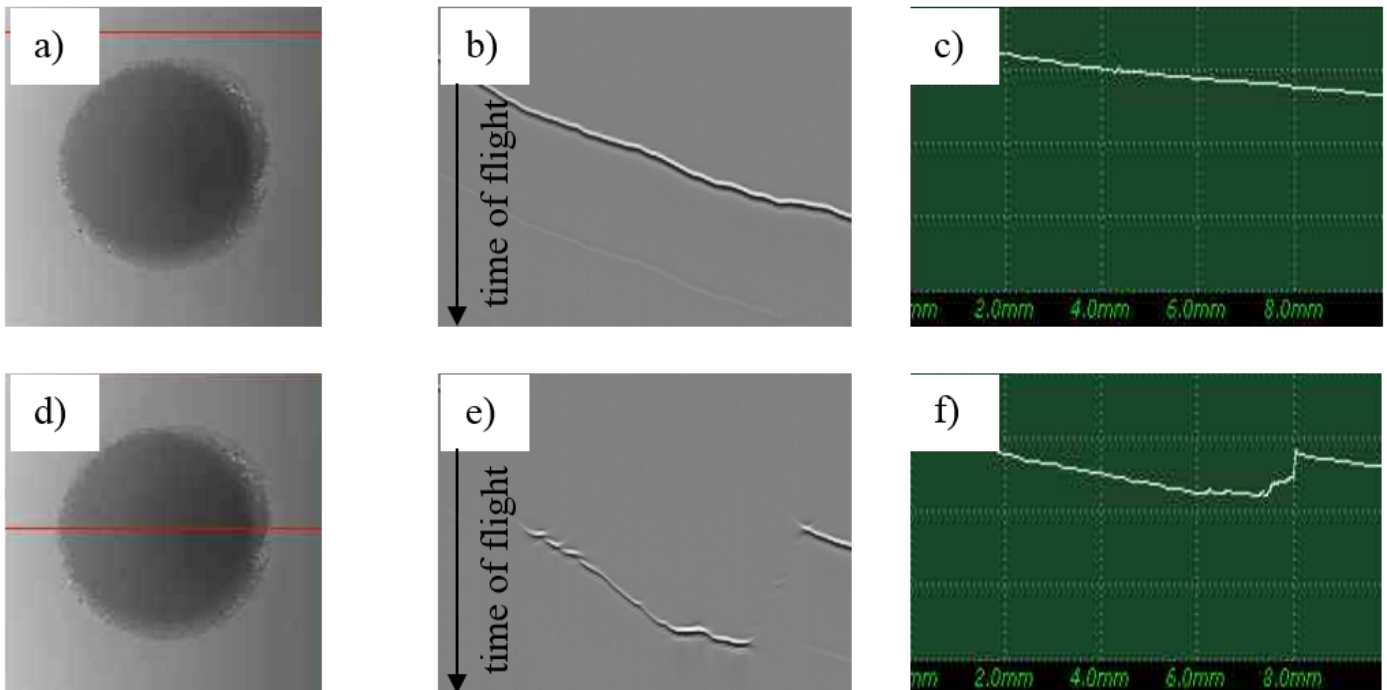


Fig. 4. The profile of the surface of the welding nugget along different cross-sections. C-scan images – (a) and (d), B-scan images – (b) and (e), graphical interpretation – (c) and (f) [8]

Scanning acoustic microscopy can be easily applied in assessment of welding joints. Schubert, Hipp and Gommlich from the Fraunhofer Institute and TU Dresden have demonstrated the ability to use scanning acoustic microscopy (SAM) and multi-transducer heads to assess the diameter of the welding nugget [9], which can be used in the initial analysis of spot-welded joints. Furthermore, it has been shown that acoustic microscopy can be

used to assess the structural changes arising inside the nugget that can be revealed using this method, which was confirmed by the presented results obtained by the authors.

Moreover, Potter, Ghaffari and Mozurkewich of the Physical and Environmental Sciences Department, Ford Research and Advanced Engineering Dearborn, Michigan, have developed a measuring system [10], which involves the use of a transducer

designed to operate in air. The results of measurements of diameter of the weld demonstrate that this can be an alternative method of measurement; however, due to discontinuities in the steel surfaces used for making the joints, the representation of the diameter of the welding nugget is less accurate than in the classical water coupling.

In addition to using the classic acoustic microscopy, tests on welds are more and more often using manual ultrasound mini-scanners. Despite their limited working space, Thornton, Han Shergold have shown [11] that the presentation of the C-scan can provide information about the shape of the welding nugget, internal discontinuities and the depth of electrodes indentation.

Moreover, a team from the University of Windsor, Ontario, Canada, used scanning microscopy to assess the joints in the nut-sheet combination [12]. Preliminary results indicate that acoustic microscopy can be used for the preliminary assessment of the quality of joints and the contact surface between the sheet and the notch. Research carried out by this team on the use of acoustic microscopy for the evaluation of welded joints, especially joints of steel is among the most advanced works in the world.

In addition to the qualitative assessment of the joints, scanning acoustic microscopy can be used to diagnose stress not only

in metallic materials. The authors [13] have used this method to evaluate the homogeneity of composite materials and silicon carbide. This method has a much broader perspective in assessing the quality of different materials.

To assess the utilitarian possibilities of scanning acoustic microscopy in this field, it is necessary to compare the results with those obtained during the conventional destructive tests using light microscopy. Only in this way will be possible to analyze the possibility of using acoustic microscopy and thus, its effectiveness to evaluate the discontinuities in welded joints.

2. Material and methods

Welded joints have been made of two grades of sheet aluminium EN AW5754 H24 (sheet thickness 1.6 mm) and EN AW6005 T606 (sheet thickness 3.5 mm). Analysis of the chemical composition of the materials is shown in Table 1. The analysis was performed by spectral analysis using a glow discharge spectroscope. Welds were made using an automatic welding machine THYSSEN OTHELFER 3DS 2-21.6-500-380-T. Table 2 shows the parameters of the welding process.

TABLE 1

The chemical composition of aluminium sheets in wt. %

Aluminium grade	Si	Mg.	Fe	Cu	Zn	Cr	Ni	Mn	Pb	Ca	Al	Ti
EN AW5754 H24	0.085	3.390	0.218	0.023	0.000	0,097	0.006	0.231	0.014	0.000	95.90	0.008
EN AW6005 T606	0.553	0.638	0.165	0.073	0.018	0.008	0.013	0.032	0.001	0.001	98.50	0.038

TABLE 2

Parameters of the welding process

Initial pressure pretime [ms]	Initial pressure time [ms]	Preheating current [kA]	Preheating time [ms]	Heat compensation time [ms]	Initial welding current value [kA]	Welding current time [ms]	Break time [ms]
520	300	3	80	320	29	120	240
Number of pulses	Cooldown time [ms]	Final reheating current value [kA]	Final reheating current time [ms]	Final holding time [ms]	Opening time [ms]	Pressing force [kN]	
1	200	6	60	500	200	2.8	

In addition, prior to welding, the material was modified, which involved: washing the sheets with ethanol (joint #2), initial polishing of joint (joint #3) and oil contamination (joint #4). This was to reflect the actual conditions on the production halls, where, despite an intense application of the 5S method (workplace organization method comprises five steps: “sort”, “straighten”, “shine”, “standardise” and “sustain”), especially in the automotive industry plants, it is still difficult to eliminate contaminants completely. In addition, the aim was to evaluate the effect of initial treatment consisting of special preparation and cleaning the surface of the welded sheets on the quality of the joints.

Prior to welding, the material was additionally modified by: washing the sheets with ethanol (joint #2), pre-polishing the

joint (joint #3), contaminating the joint with oil (joint #4), filing the sheets (joint #5) and cooling the sheets to a temperature of 0°C (joint #6).

Research using scanning acoustic microscopy was performed with a device designed and manufactured at the Department of Materials Science, Welding and Strength of Materials at the Faculty of Mechanical Engineering of the Technical University of Wrocław. The acoustic microscope comprises three independently-controlled axes, whose function is to move the transducer (axes X and Z) and the test object (Y-axis). The transducer’s movement relative to the Z-axis is used to determine the distance of the transducer relative to the tested object. For a transducer with beam focusing, Z-axis is used to determine the distance of the focus from the surface.

All measurements were performed using the following parameters:

- oscillation frequency of the transducer: 20 MHz,
- focus length in water: 15 mm,
- focus size: 0.5 mm,
- resolution in axes x-y: 50 μm ,
- greyscale: 256,
- scan area: 12 \times 12 mm.

The control system of individual axes and triggering of the ultrasonic signal is implemented in software through a PC coupled with a microprocessor control system via a USB-RS232 bus. Scanning parameters are set using a GUI, which is an integral part of the scanner.

In addition to visualizing the continuity area of the weld in a plane parallel (C-scan) and perpendicular (B-scan) to the surface, the developed measuring system allows measuring the diameter and indentation depth of the electrodes.

Scanning acoustic microscopy allows making a large number of cross-sections in the direction perpendicular to the sample surface. Their number is the result of only the initial conditions, which consist of the resolution in the Y-axis. It should be noted that in getting the metallographic composition corresponding to the B-scan requires grinding the sample to the desired cross-section. The example C-scan presentation of the joint and the corresponding B-scan cross-sections are presented in Fig. 5.

Macroscopic study of the joint was made using a stereo microscope SMT-800.

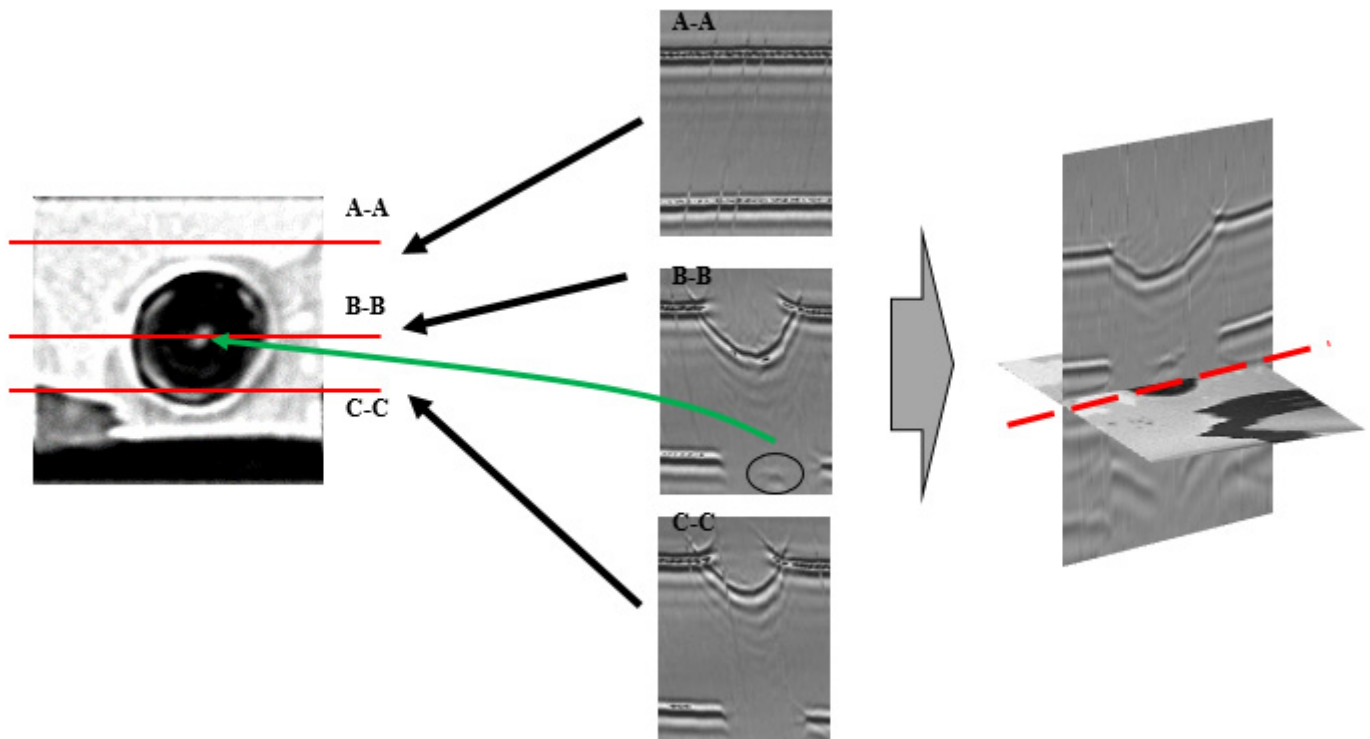


Fig. 5. Interpretation of ultrasound signals B- and C-scan

Microscopic observation was carried out after chemical etching. Chemical reagents for aluminium alloys according to PN-H-04512:1975 were used to reveal the microstructure. To observe the microstructure, a Neophot 32 light microscope was used. Microscopy images of microstructures were recorded with a microscope coupled to a Visitron Systems digital camera using Spot Advanced software.

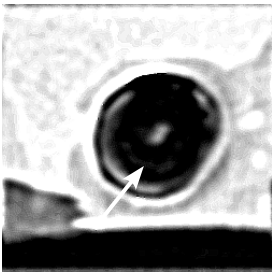
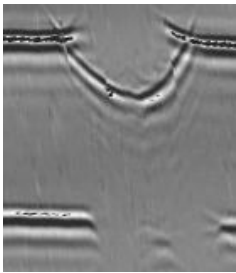
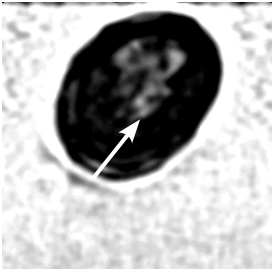
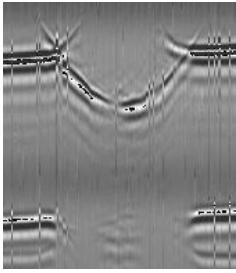
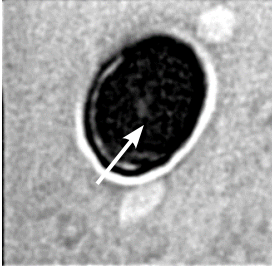
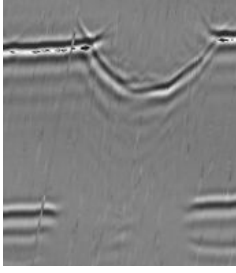
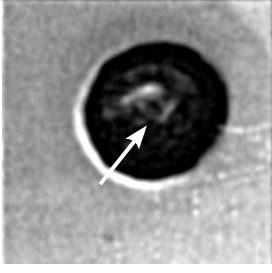
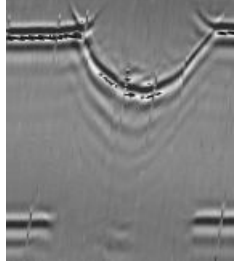
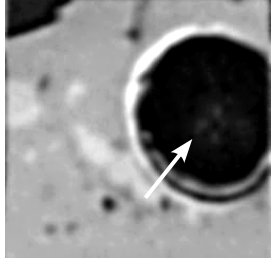
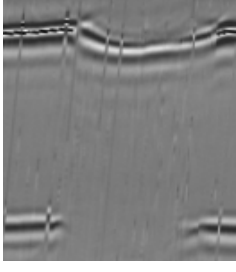
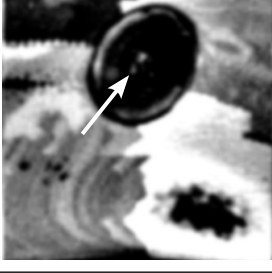
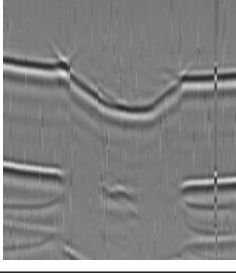
3. Results

Table 3 shows the results of acoustic microscopy testing of spot welded joints. The column labelled C-scan shows ultrasonic cross-sections parallel to the surface of the joined

sheets at the point of contact. The column labelled B-scan shows cross-sections perpendicular to the sheet surface, made in the axis of the joint. In Figures 6 to 16 show the results of destructive testing.

A clear advantage of acoustic microscopy is the ability to very accurately map the shape of the weld joint, whose analysis by metallographic study is possible only in one cross-section perpendicular to the sheet surface. The findings indicate that the joints designated 1.4 and 5 in a direction parallel to the surface have a circular shape while joints 2.3 and 6 are oval. These differences may be due to the different wear condition of the electrodes. Furthermore, some discontinuities were revealed in the joints, which are then analyzed by means of destructive tests.

Collective results of ultrasonic testing of spot welds. Arrows indicate discontinuities in joints

Joint No.	C-scan	B-scan	Diameter [mm]	Indentation [mm]
1			6.08	0.27
2			8.53	0.27
3			5.01	0.28
4			6.3	0.29
5			6.9	0.11
6			5.2	0.15

Joint No. 1 not subject to modification

The shape of the welding nugget – similar to a lens is adequate to the temperature gradient present in the area of the spot-welded joint. It is high in the direction of the electrodes supplying the welding current (due to their high thermal conductivity), but becomes much smaller in the direction of the base material, whose thermal conductivity is lower (Fig. 6).

It should be noted that from a metallurgical point of view, the solidification of liquid metal is similar to metallurgical ingots [14]. The crystallization process begins with a homogeneous substrate, upon which unmelted material is welded. There is the ‘so-called’ competitive grain growth stage, which involves the fact that their lengths are governed by the compliance of the crystallographic orientation of the substrate with the direction of the most intense heat transfer. Crystals in which this compliance does not occur are subject to the ‘so-called’ interlock, which is referred to as the epitaxial grain growth.

The factor that effects on the structure of the joint area is the intensity of cooling. Excessive heat transfer to the electrodes (caused e.g. by overcooling) induces the formation of long pillar-like crystals oriented in the direction of the electrode [15]. Due to the rapid dissipation of heat in the vertical direction (towards the electrode); the welding nugget has a relatively smaller size. At the same time, the central portion at the interface with the base material shows increased risk of cracks and shrinkage cavities [16]. If the temperature gradient is greater in the direction of the welded material – e.g. in case of electrode overheating or a small

interface between the electrode and the material, the pillar-like crystals are oriented in the direction of the welded material.

As a result of destructive tests in a weld joint, pores were found with a maximum diameter of approx. 0.13 mm (Fig. 7b) and a crack propagating in both in the direction of the metal sheet made of aluminium alloy EN AW5754 H24 and EN AW6005 T606 (Fig. 7c and 7d). In addition, the heat affected zone shows microcracks propagating along the grain boundaries of the α phase of alloy EN AW6005 T606. The penetration area consists of pillar-like crystals while in the welding nugget; the structure is consists of equiaxed dendrites (Fig. 7a). The crystal area is larger on the side of metal alloy EN AW5754 H24 (approx. 0.30 mm) than in the metal alloy EN AW6005 T606 (approx. 0.10 mm), which shows the directional crystallization and thermal conductivity of alloy sheet EN AW5754 H24. In the welding nugget, micropores were observed in interdendritic areas.

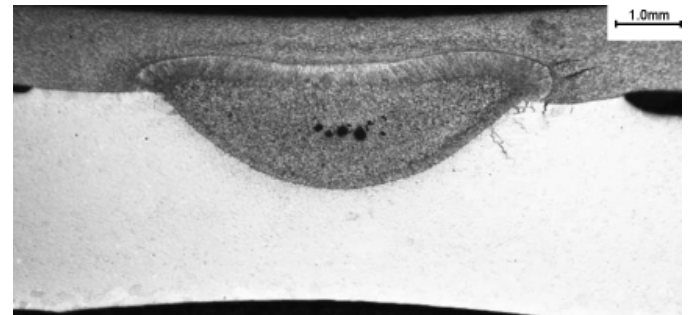


Fig. 6. General view of the weld joint with visible cracks and porosity in the welding nugget, etched with Ma1Al

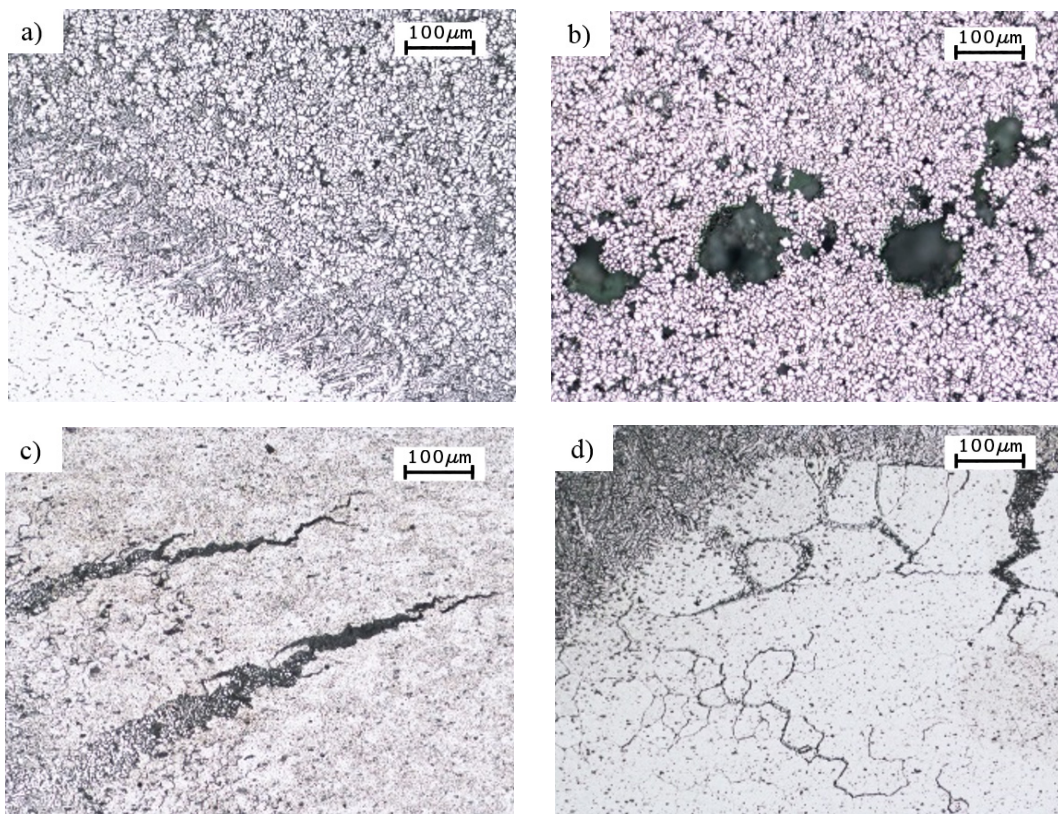


Fig. 7. a) penetration area and welding nugget; b) porosity in the welding nugget; c) cracks in sheet EN AW5754 H24; d) cracks in sheet EN AW6005 T606, etched with Ma1Al

Joint No. 2 – sheet metal degreased with ethanol

Degreasing sheets with ethanol before the welding process did not improve the quality of the welds. Just as in the weld not subjected to the modification, cracks were observed (a length of up to approx. 0.8 mm) propagating both in the direction of metal sheet made of aluminium alloy EN AW5754 H24 and EN AW6005 T606, where they propagate along the grain boundaries of phase α (Fig. 9a). The penetration area is a zone of pillar-like crystals that is larger on the side of sheet alloy EN AW5754 H24 (approx. 0.30 mm) than sheet alloy FR AW6005 T606 (approx. 0.10 mm) (Fig. 8). In the welding nugget there is a equiaxed dendritic structure and numerous discontinuities in the form of pores with a diameter reaching up to 0.13 mm (Fig. 9b), micro-

cracks along the dendrite boundary and micropores derived from interdendritic spaces.

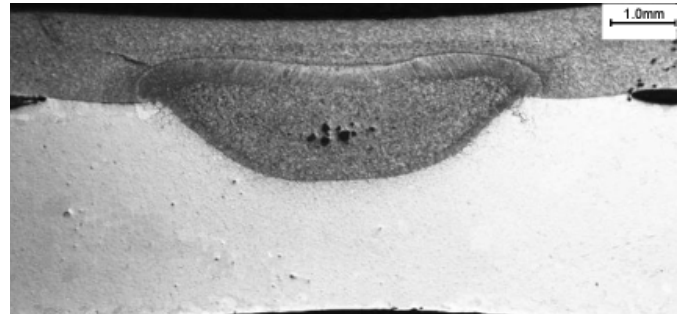


Fig. 8. General view of the weld joint with visible cracks and porosity in the welding nugget, etched with Ma1Al

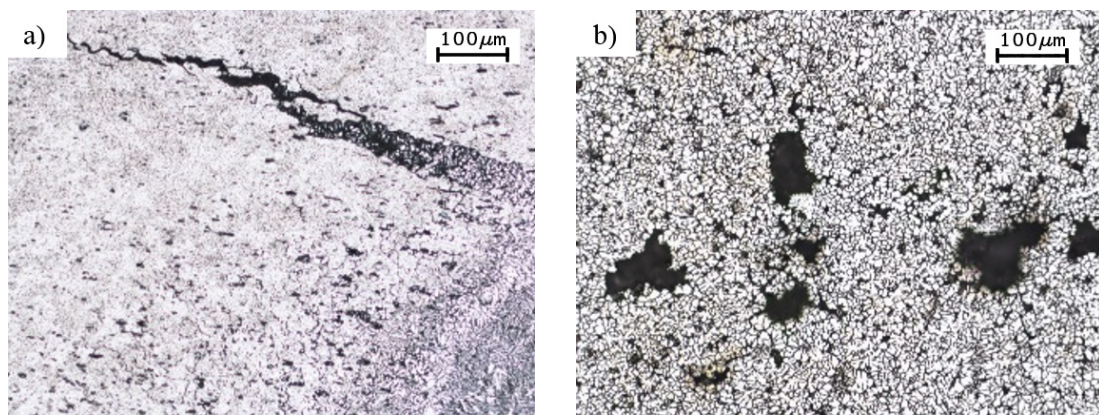


Fig. 9. a) cracks in sheet EN AW5754 H24; b) porosity in welding nugget, etched with Ma1Al

Joint No. 3 – pre-polished sheets

Just as degreasing, additional pre-polishing treatment of the sheet brought no improvement in the quality of the welds. Conventional destructive tests showed a large number of cracks in the heat affected zone, propagating in the direction of the two sheets (Fig. 10). In the centre of the nugget, on the other hand, there are a few large pores the size of up to 0.18 mm and smaller discontinuities, such as cracks extending along the dendrite boundary, and smaller pores in the interdendritic spaces. The structure of the joint is typical, lens-shaped, with a distinctive crystal zone, wider on the side of sheet made of alloy EN AW5754 H24.

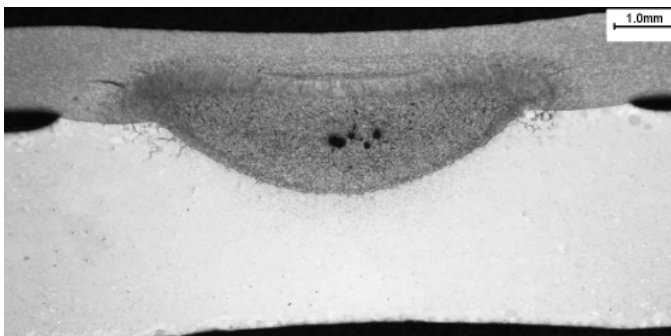


Fig. 10. General view of the weld joint with visible cracks and porosity in the welding nugget, etched with Ma1Al

Joint No. 4 – sheets contaminated with oil

Contaminating the metal with oil was also aimed at analyzing its impact on the quality of welded joints. During macroscopic testing, the nugget was shown to have deviated slightly from the contact plane (Fig. 11). Cracks (with the length of up to approx. 0.7 mm) propagate in both the metal sheet made of aluminium alloy EN AW5754 H24 (Fig. 12a) and EN AW6005 T606, which propagate along the grain boundaries of phase α (Fig. 12b). The penetration area consists of pillar-like crystals. The crystal area is larger on the side of sheet alloy EN AW5754 H24 (approx. 0.30 mm) than sheet alloy FR AW6005 T606 (approx. 0.10 mm). Microscopic tests revealed that the weld-

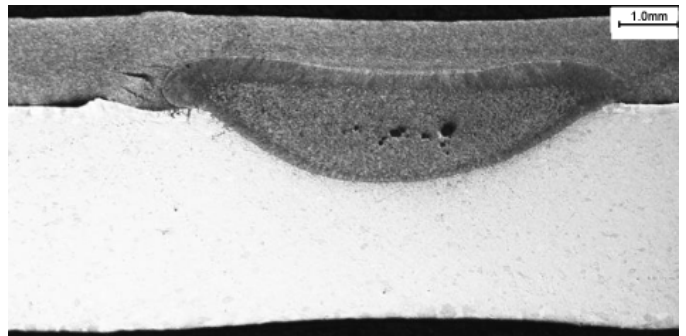


Fig. 11. General view of the weld joint with visible cracks and porosity in the welding nugget, etched with Ma1Al

ing nugget has a equiaxed dendritic structure, and a number of discontinuities were identified in the form of pores the size of up to 0.15 mm, microcracks along the dendrite border, and micropores having derived from the interdendritic areas. Fur-

thermore, oil particles have been identified, which are also the source of discontinuities weakening the analyzed joint. Due to diffusion, oil particles have even been pushed in the area of the base material (Fig. 12a).

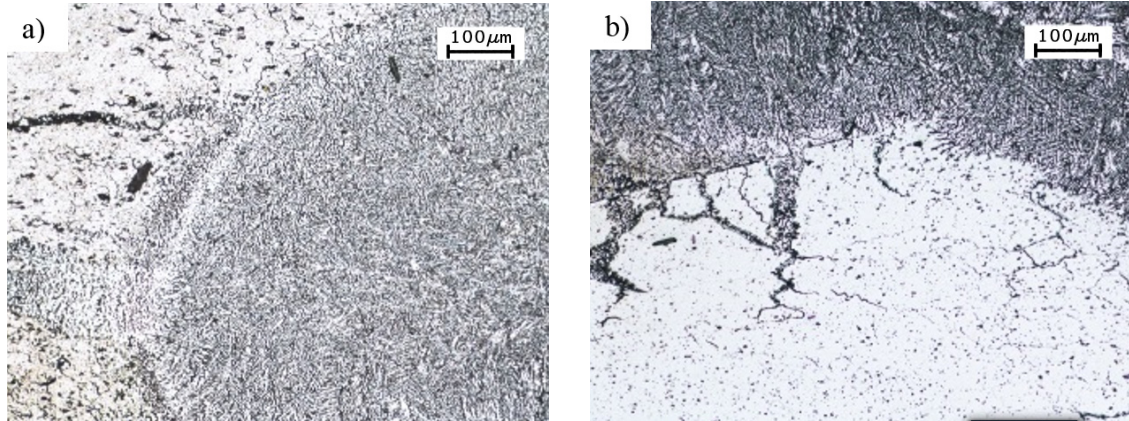


Fig. 12. a) cracks in sheet EN AW5754 H24 with visible oil particles; b) cracks in sheet EN AW5754 H24, etched with Ma1Al

Joint No. 5 – sheets contaminated with metal filings

Contaminating sheets with metal filings resulted in significant deterioration in the quality of the resulting weld joint. This was apparent especially in the nugget, where an accumulation of discontinuities was observed in the form of numerous large pores with diameters of up to 0.18mm, as well as, small pores localized in the interdendritic areas (Fig. 13). In some discontinuities metal particles may be observed. This finding means that the presence of contaminants caused much deterioration in the joints (Fig. 14a). The welding nugget area occupied by discontinuities is 15%. Cracks (with the length of up to approx. 0.8 mm) propagate in both the sheet made of aluminium alloy EN H24 AW5754 and AW6005 FR T606; where they propagate along the grain boundaries of phase α (Fig. 14b). The structure of the connector shows a clear zonation. The fusion area contains pillar-like crystals. The crystal zone is larger on the side of sheet made of alloy EN AW5754 H24 than the sheet made of alloy EN

AW6005 T606. In the case of sheet H24 AW5754, the thickness of the zone itself is varied, ranging from 0.15 mm to 0.30 mm. However, in the case of sheet FR AW6005 T606, the thickness is fixed at about 0.10 mm. The welding nugget has an equiaxed dendritic structure.

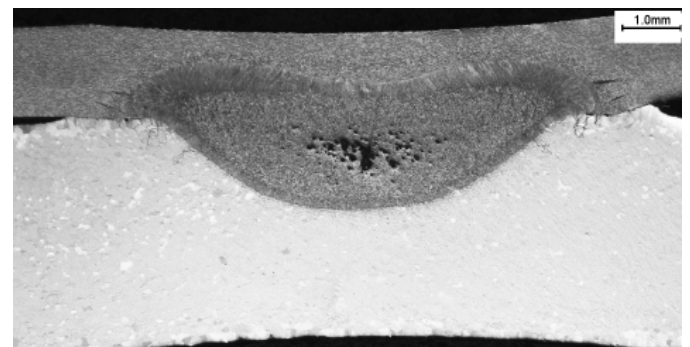


Fig. 13. General view of the weld joint with visible cracks and porosity in the welding nugget, etched with Ma1Al

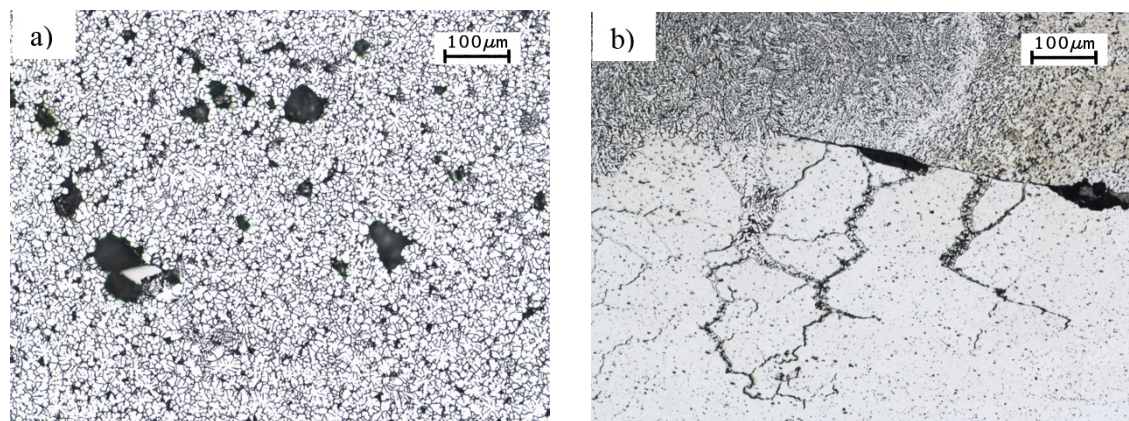


Fig. 14. a) porosity in the welding nugget; b) cracks in sheet EN AW6005 T606; etched with Ma1Al

Joint No. 6 – sheets cooled to 0°C

Pre-cooling the sheets to 0°C was additionally aimed at determining the effect of temperature on the quality of welded joints. Based on macroscopic testing, a discrepancy was identified in the form of nugget deviations from interface (i.e. nugget asymmetry). Moreover, the interface between sheets shows signs of adhesion (Fig. 15).

The heat affected zone shows cracks propagating in the direction of sheet alloy EN AW6005 T606 with a length of approx. 0.20 mm (Fig. 16b). The centre of the nugget contains pores with a diameter of 0.13 mm and a number of smaller discontinuities in the form of cracks running along the border of dendrites and smaller pores (Fig. 16a).

The fusion area contains pillar-like crystals. The pillar-like crystal zone is greater on the side of sheet made of alloy EN AW5754 H24 (approx. 0.30 mm) than the sheet FR AW6005

T606 (approx. 0.10 mm). As in joint No. 1, which was not subjected to modifications, the welding nugget contains dendrites and pores originating in the interdendritic spaces.

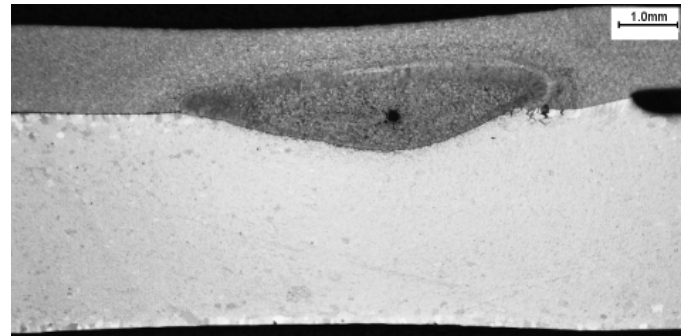


Fig. 15. General view of the weld joint with visible cracks and porosity in the welding nugget, etched with Ma1Al

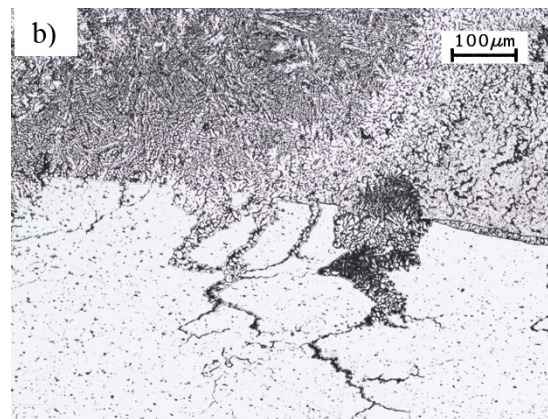
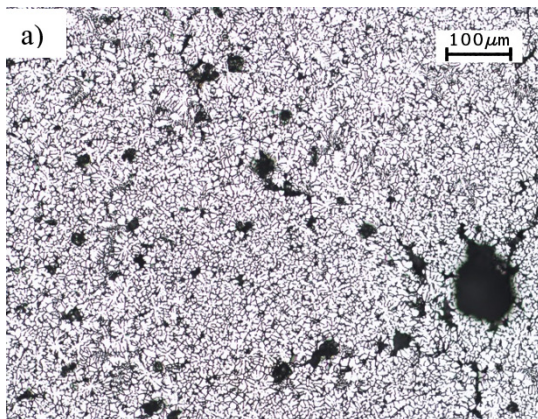


Fig. 16. a) porosity in the welding nugget; b) cracks in sheet EN AW6005 T606; etched with Ma1Al

4. Conclusion

Non-destructive testing of spot welded joints made of aluminium alloys have long been an important area of materials science. The results obtained by the authors fit substantially into the trends in current scientific papers and publications, and confirm the possibility of using this method for the assessment of discontinuities in welded joints.

Already the first publication of this subject, dating as far back as the late 1990's had raised high hopes associated with the development of control techniques [17]. In subsequent years, scanning acoustic microscopy has become a common method for non-destructive testing, and the use of the presentation of B- and C-scan allowed for the identification of such discontinuities as voids and foreign inclusions [7]. Automatic evaluation and identification of discontinuities is made possible by the use of neural network algorithms [18].

Based on the research, it was demonstrated that all of the tested joints have internal discontinuities in the central part, as shown on ultrasound cross-sections, i.e. C-scan and B-scan presentations. Moreover, for joints 3 and 4 on the side of the weld

perimeter there was weaker acoustic feedback (shown as light bands), which may indicate the adhesive nature of the joint, the so-called gluing. Due to the relatively low resolution resulting mainly from the size of the focus, this is a qualitative assessment, which, however, confirms the metallographic micro- and macroscopic tests. The study indicates that the ultrasonic scanning microscopy can be used to test materials in welded joints both in terms of measuring the actual penetration surface in the joined sheets, as well as to show internal discontinuities such as voids and pores. Its big advantage is the possibility of obtaining any (albeit limited by the central unit's memory) number of cross-sections perpendicular to the surface of the joint. The only discontinuities, which are not shown in ultrasonic scanning microscopy, were microcracks.

Additionally, it is noted that contaminating metal with oil, or pre-treatment of sheets through their cleaning or polishing does not affect the quality of the resulting weld.

Acknowledgments

This paper is based on research funded by National Centre of Research and Development as part of project no. PBS3/B4/12/2015 entitled: "Development of innovative compact high-efficient higher frequency welder".

REFERENCES

- [1] S. Stano, *Welding Institute Bulletin* **2**, 24-25 (2005).
- [2] H. Papkała, A. Pietras, L. Zadroga, *Welding Technology Review* **5-7**, 51-57 (2004).
- [3] Y. Cho, I. Chang, H. Lee, *Welding J.* **85** (8), 26-29 (2007).
- [4] R. Gr. Maev, F. Severin, Acoustic Microscope Inspection of Cylindrical Butt Laser Welds, in: M.P. Andre, J.P. Jones, H. Lee (Ed.), *Acoustical Imaging* **30**, Springer Science + Business Media B.V. (2011).
- [5] E. Drescher-Krasicka, C.P. Ostertag, *J. Mater. Sci.* **34**, 4173-4179, (1999).
- Y.V. Korkh, D.V. Perov, A.B. Rinkevich, *Acoustic Methods Russian Journal of Nondestructive Testing*, **51** (4), 198-209 (2015).
- [6] G.M. Crean, C.M. Flannery, S.C.Ó. Mathúna, Acoustic Microscopy Analysis of Microelectronic Interconnection and Packaging Technologies, in: A. Briggs (Ed.), *Advances in Acoustic Microscopy* **1**, Plenum Press 1995.
- [7] A.M. Chertov, R.G. Maev, F.M. Severin, *IEEE Transactions on Ultrasonics, Ferroelectrics, and Frequency Control* **54** (8), 1521-1529 (2007).
- [8] M. Korzeniowski, *Monitoring by Ultrasonic Method Resistance Welding Process*. PhD thesis, Wrocław University of Technology, Wrocław, September 2008, in Polish.
- [9] F. Schubert, R. Hipp, A. Gommlich, Determination of Diameter and Thickness of Weld Nuggets in Resistance Spot Welding by High Frequency Ultrasound Inspection, *Proceeding on 11th European Conference on Non-Destructive Testing (ECNDT 2014)*, Prague, Czech Republic (2014).
- [10] T.J. Potter, B. Ghaffari, G. Mozurkewich, *NDT&E International* **38** (5), 374-380 (2005).
- [11] M. Thornton, L. Han, M. Shergold, *NDT&E International* **48**, 30-38 (2012).
- [12] R. Gr. Maev, F. Seviaryn, Ultrasonic Imaging Inspection of Projection Welds, *Proceeding on 5th Pan American Conference for NDT Cancun, Mexico* (2011).
- [13] J.T. Bonarski, L. Tarkowski, S. Pawlak, A. Rakowska, Ł. Major, *Arch. Metall. Mater.* **59** (2), 437-441 (2014).
- [14] H. Papkała, *Resistance Welding of Metals*, WiHK „KaBe” s.c. Krosno 2003.
- [15] H. Zhang, J. Senkara, *Resistance Welding Fundamentals and Application*, CRC Press Taylor&Francis Group 2006.
- [16] A. Jaquin, A.N.A. Elliott, Ch. Jiang, *Welding J.* **86** (2), 24-27 (2007).
- [17] R. Gr. Maev, D.F. Watt, R. Pan, V.M. Levin, K.I. Maslov, *Acoustical Imaging* **22**, 779-784 (1996).
- [18] H.T. Lee, M. Wang, R.G. Maev, E. Maeva, *Int. J. Adv. Manuf. Technol.* **22**, 727-732 (2003).